Journal of Organometallic Chemistry 695 (2010) 1146–1154

Contents lists available at ScienceDirect

Journal of Organometallic Chemistry

journal homepage: www.elsevier.com/locate/jorganchem

Mixed-metal cluster synthesis: $[Re(CO)_3(\mu\text{-}S_2NC_7H_4)]_2$ as a precursor for tri- and tetranuclear 2-mercaptobenzothiolato capped clusters

Shishir Ghosh [a], Kamrun N. Khanam [a], Md. Kamal Hossain [a], G.M. Golzar Hossain [b], Daniel T. Haworth [c,1], Sergey V. Lindeman [c], Graeme Hogarth [d], Shariff E. Kabir [a,*]

[a] Department of Chemistry, Jahangirnagar University, Savar, Dhaka 1342, Bangladesh
[b] Department of Chemistry, Dhaka University, Dhaka 1000, Bangladesh
[c] Department of Chemistry, Marquette University, P.O. Box 1881, Milwaukee, WI 53201-1881, USA
[d] Department of Chemistry, University College London, 20 Gordon Street, London WC1H 0AJ, UK

ARTICLE INFO

Article history:
Received 23 December 2009
Received in revised form 14 January 2010
Accepted 15 January 2010
Available online 25 January 2010

Keywords:
Mixed-metal cluster
Carbonyls
2-Mercaptobenzothiazole
X-ray structures

ABSTRACT

The readily prepared $[Re_2(CO)_6(\mu\text{-}S_2NC_7H_4)_2]$ (**1**) reacts with Group 8 trimetallic carbonyl clusters to yield new mixed-metal tri- and tetranuclear clusters. With $[Os_3(CO)_{10}(NCMe)_2]$ at 80 °C the tetranuclear mixed-metal cluster $[Os_3Re(CO)_{13}(\mu_3\text{-}C_7H_4NS_2)]$ (**2**) is the only isolated product. With $Ru_3(CO)_{12}$ products are dependent upon the reaction temperature. At 80 °C, a mixture of tetranuclear mixed-metal $[Ru_3Re(CO)_{13}(\mu_3\text{-}C_7H_4NS_2)]$ (**5**) and the triruthenium complex $[Ru_3(CO)_9(\mu\text{-}H)(\mu_3\text{-}C_7H_4NS_2)]$ (**4**) results, while at 110 °C a second tetranuclear mixed-metal cluster, $[Re_2Ru_2(CO)_{12}(\mu_4\text{-}S)(\mu\text{-}C_7H_4NS)(\mu\text{-}C_7H_4NS_2)]$ (**3**), resulting from carbon–sulfur bond scission, is the major product. Reaction of **1** With $Fe_3(CO)_{12}$ at 80 °C furnishes the trinuclear mixed-metal cluster $[Fe_2Re(CO)_8(\mu\text{-}CO)_2(\mu_3\text{-}C_7H_4NS_2)]$ (**6**). The reactivity of **6** has been probed with the aim of identifying any metal-based selectivity for carbonyl substitution. Addition of PPh_3 in presence of Me_3NO at 25 °C gives both the mono- and bis(phosphine)-substituted derivatives $[Os_3Re(CO)_{12}(PPh_3)(\mu_3\text{-}C_7H_4NS_2)]$ (**7**) and $[Os_3Re(CO)_{11}(PPh_3)_2(\mu_3\text{-}C_7H_4NS_2)]$ (**8**). In **7** the PPh_3 ligand occupies an axial site on wingtip osmium, while in **8** one PPh_3 ligand is equatorially coordinated to wingtip osmium and the other is bonded to a hinge osmium. New complexes have been characterized by a combination of spectroscopic data and single crystal X-ray diffraction studies.

1. Introduction

The chemistry of mixed-metal clusters has been studied in great detail in recent years [1,2] since compounds containing disparate metals in close proximity can be used as models for the surface of heterogeneous catalysts [3–6]. The incorporation of different metal types in clusters may also have synergistic effects for catalytic transformation and indeed recently they have been employed in homogeneous catalysis [3,7–9]. Further, mixed-metal clusters have non-equivalent bonding sites and offer the possibility of combining catalytic features of different metal centers [10,11].

The development of suitable synthetic routes to mixed-metal clusters of desired structural and reactivity features remains a major challenge. Displacement reactions of metal carbonyl anions with metal halides are the most predictable and widely used method. Others routes include the combination of a metal carbonyl anion and a neutral metal carbonyl or co-pyrolysis of different homometallic carbonyl units. In early nineties, Deeming et al. prepared a series of rhenium–ruthenium clusters containing $ReRu_3$, Re_2Ru_2 and $ReRu_3$ cores in a rather simple way from the reaction of $[Re_2(CO)_6(\mu\text{-}pyS)_2]$ with $Ru_3(CO)_{12}$ in refluxing xylene, thereby establishing that the dinuclear $[Re_2(CO)_6(\mu\text{-}pyS)_2]$ is an excellent source for the incorporation of an $[Re(CO)_3(pyS)]$ unit into the trimetallic system [12]. More recently we have developed this approach, taking advantage of the lability of the metal–sulfur bond in $[M_2(CO)_6(\mu\text{-}L)_2]$ (M = Re, Mn; L = heterocyclic thiol) [13]. Thus we have prepared $[CpMoMn(CO)_3(\mu\text{-}CO)(\mu\text{-}\eta^2\text{-}pyS)(\mu\text{-}\eta^1\text{-}pyS)]$ [14] from the reaction of $[Mn_2(CO)_6(\mu\text{-}pyS)_2]$ and $[CpMo(CO)_3]_2$ at 110 °C, obtained a series of Group 6/7 mixed-metal complexes $[MMn_2(CO)_8(\mu\text{-}CO)_2(\mu_3\text{-}SN_2C_4H_5)]$ (M = W, Mo, Cr) from reactions of $[Mn_2(CO)_6(\mu\text{-}SN_2C_4H_5)_2]$ and $[M(CO)_3(NCMe)_3]$ and synthesised Group 7/8 mixed-metal clusters $[M_3M'(CO)_{13}(\mu_3\text{-}SN_2C_4H_5)]$ (M = Os, Ru; M′ = Mn, Re) from $[M_3(CO)_{12-x}(NCMe)_x]$ (x = 0, 2) and $[M'_2(CO)_6(\mu\text{-}SN_2C_4H_5)_2]$ [15,16] (Chart 1). Further developing this approach, herein we describe reactions of the dirhenium 2-mercaptobenzothiazolato complex, $[Re_2(CO)_6(\mu\text{-}S_2NC_7H_4)_2]$ (**1**), with $[M_3(CO)_{10}L_2]$ (M = Os, Ru, Fe; L = CO, MeCN) leading to the formation of tri- and tetranuclear mixed-metal clusters. We also present some preliminary reactivity studies of a mixed rhenium–

* Corresponding author. Tel.: +406 243 2592; fax: +406 243 2477.
E-mail address: skabir_ju@yahoo.com (S.E. Kabir).

[1] D.T. Haworth died on July 6, 2009, at the age of 81, following a recent diagnosis of cancer.

0022-328X/$ - see front matter © 2010 Elsevier B.V. All rights reserved.
doi:10.1016/j.jorganchem.2010.01.021

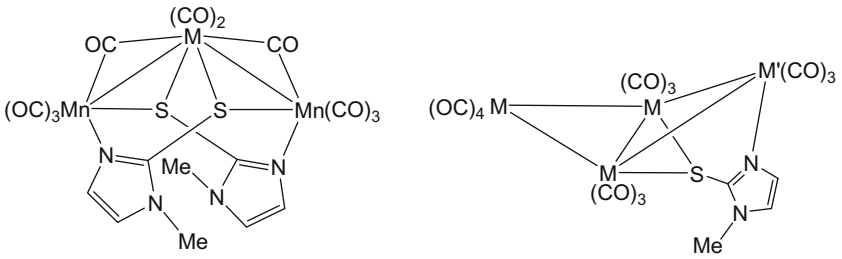

Chart 1.

osmium cluster with PPh_3. The striking feature of this study is the formation of mixed-metal clusters that differ in both nuclearity and structural features when using different Group 8 carbonyls, which relates to a strong influence of the intrinsic reactivity of the metal carbonyls during these transformations.

2. Results and discussion

2.1. Preparation of dirhenium 2-mercaptobenzothiazolato complex $[Re_2(CO)_6(\mu\text{-}S_2NC_7H_4)_2]$ (**1**)

In a method analogous to that reported by Deeming et al. for the synthesis of the pyridine-2-thiolato complex $[Re_2(CO)_6(\mu\text{-}pyS)_2]$ [13] we prepared $[Re_2(CO)_6(\mu\text{-}S_2NC_7H_4)_2]$ (**1**) in 66% yield from the Me_3NO-initiated reaction of $Re_2(CO)_{10}$ with 2-mercaptobenzothiazole at 25 °C. An ORTEP diagram of the molecular structure of **1** is depicted in Fig. 1, the caption containing selected bond distances and angles. The molecule adopts a chiral structure with C_2 symmetry being similar to that of pyridine-2-thiolato dirhenium complex $[Re_2(CO)_6(\mu\text{-}MepyS)_2]$ [13]. Each 2-mercaptobenzothiazolato ligand bridges the dirhenium center through the sulfur, while the nitrogen coordinates to a single metal atom thus forming a four-membered chelate ring. The Re_2S_2 ring is non-planar with a dihedral angle of 30.25(4)° between Re_2S planes. The three carbonyls on each rhenium are arranged in a facial fashion and assuming the 2-mercaptobenzothiazolato ligand serves as five-electron donor both rhenium centers achieves 18-electron configuration without any metal–metal bond [Re(1)···Re(1′) 3.7543(5) Å]. Spectroscopic data are consistent with the solid-state structure.

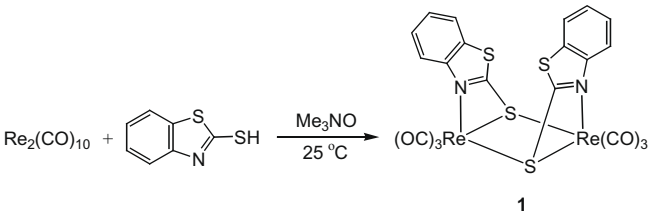

1

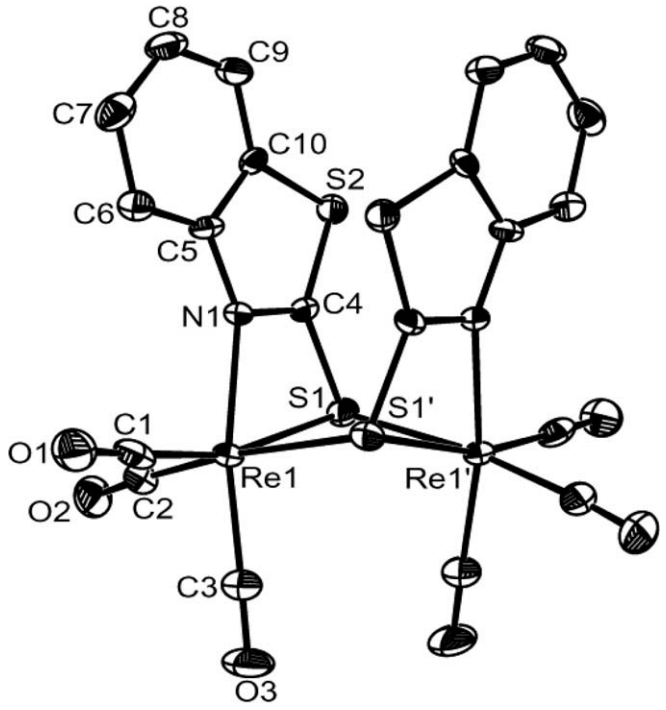

Fig. 1. ORTEP diagram of the molecular structure of $[Re_2(CO)_6(\mu\text{-}S_2NC_7H_4)_2]$ (**1**), showing 50% probability thermal ellipsoids. Selected interatomic distances (Å) and angles (°): Re(1)–C(1) 1.905(8), Re(1)–C(2) 1.908(7), Re(1)–C(3) 1.929(7), Re(1)–N(1) 2.160(5), Re(1)–S(1) 2.589(2), Re(1)–S(1′) 2.542(2), C(1)–Re(1)–C(2) 91.1(3), C(1)–Re(1)–C(3) 89.7(3), C(2)–Re(1)–N(1) 96.0(3), C(3)–Re(1)–N(1) 169.1(3), N(1)–Re(1)–S(1′) 87.6(2), S(1′)–Re(1)–S(1) 82.32(5), Re(1′)–S(1)–Re(1) 94.03(5).

2.2. Synthesis of mixed-metal clusters

In an attempt to utilize **1** towards the synthesis of a range of mixed-metal clusters it was heated with the group 8 carbonyls $M_3(CO)_{12}$ (M = Fe, Ru) and $[Os_3(CO)_{10}(MeCN)_2]$ with the expectation of forming tetranuclear complexes of the type $[M_3Re(\text{-}CO)_{13}(\mu_3\text{-}C_7H_4NS_2)]$. The results of these studies are summarized in Scheme 1. Most successful in this respect was the reaction with $[Os_3(CO)_{10}(NCMe)_2]$ which proceeded smoothly in refluxing benzene to afford $[Os_3Re(CO)_{13}(\mu_3\text{-}C_7H_4NS_2)]$ (**2**) in 61% yield. An ORTEP drawing of the molecular structure of **2** is depicted in Fig. 2, the caption containing selected bond distances and angles. The molecule contains a tetranuclear core of one rhenium and three osmium atoms ligated by thirteen carbonyls and a 2-mercaptobenzothiazolato ligand. The four metal atoms form a butterfly skeleton where the rhenium occupies a wingtip position. All carbonyls are all terminal. The 2-mercaptobenzothiazolato ligand caps the $ReOs_2$ triangle and contains a non-crystallographic mirror plane of symmetry. Among the five different metal–metal bond lengths the hinge osmium–osmium vector is the shortest, but all distances are within the range expected for osmium–osmium and osmium–rhenium single bonds [16–18].

The reaction with $Ru_3(CO)_{12}$ was not so clean. When carried out in refluxing benzene, two products were isolated, namely the known triruthenium complex $[Ru_3(CO)_9(\mu\text{-}H)(\mu_3\text{-}C_7H_4NS_2)]$ [19] (**3**) and the new butterfly cluster $[Ru_3Re(CO)_{13}(\mu_3\text{-}C_7H_4NS_2)]$ (**4**) in 14 and 23% yields, respectively. Cluster **3** has previously been reported by Jeannin et al., being obtained from the direct reaction of $Ru_3(CO)_{12}$ and 2-mercaptobenzothiazole, and was structurally characterized [19]. Here it is formed as a result of transfer of the 2-mercaptobenzothiazolato ligand from rhenium to ruthenium.

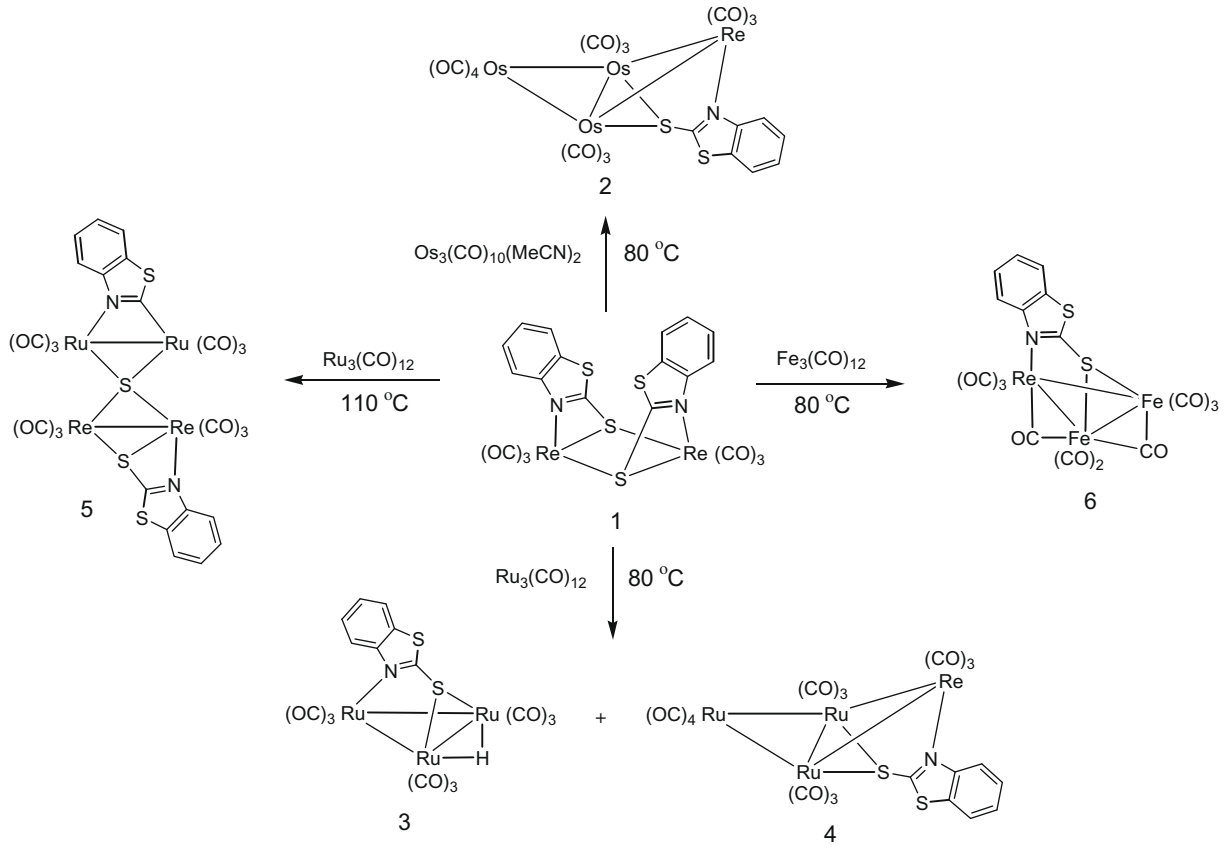

Scheme 1.

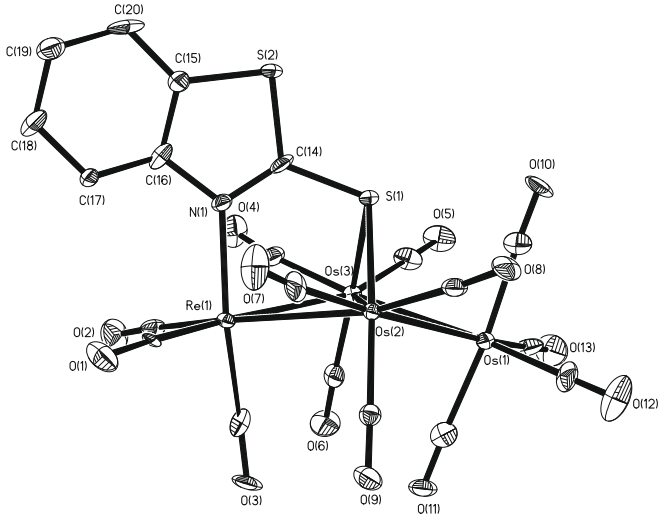

Fig. 2. ORTEP diagram of the molecular structure of $[Os_3Re(CO)_{13}(\mu_3\text{-}C_7H_4NS_2)]$ (**2**), showing 50% probability thermal ellipsoids. Selected interatomic distances (Å) and angles (°): Os(1)–Os(2) 2.8474(7), Os(1)–Os(3) 2.8629(7), Os(2)–Os(3) 2.7814(6), Os(2)–Re(1) 2.8939(7), Os(3)–Re(1) 2.9539(7), Os(2)–S(1) 2.416(3), Os(3)–S(1) 2.406(3), Re(1)–N(1) 2.194(9), Os(2)–Os(1)–Os(3) 58.297(14), Os(3)–Os(2)–Os(1) 61.130(17), Os(3)–Os(2)–Re(1) 62.693(16), Os(2)–Os(3)–Os(1) 60.573(17), Os(1)–Os(2)–Re(1) 119.081(18), Os(2)–Os(3)–Re(1) 60.519(17), Os(2)–Re(1)–Os(3) 56.788(14), Os(1)–Os(3)–Re(1) 116.593(19), Os(3)–S(1)–Os(2) 70.46(7), C(3)–Re(1)–N(1) 174.2(4), S(1)–Os(2)–Os(3) 54.61(6), S(1)–Os(2)–Os(1) 83.82(6), S(1)–Os(3)–Os(2) 54.93(6).

The new mixed-metal cluster **4** was the anticipated reaction product and is analogous to **2**. It has been characterized by a combination of spectroscopic data and single crystal X-ray diffraction analysis. The latter suggests that **4** is actually an isomorphous mixture of two isomers – one with rhenium coordinated by nitrogen atom and another where rhenium bears four carbonyls and the ratio is approximately 2:1. In the ORTEP diagram Re(1) goes with Ru(2) which is 64% (**4a**) and Ru(1) goes with Re(2) which is 36% (**4b**) (Chart 2). An ORTEP diagram of the major isomer is shown in Fig. 3. The empirical formula in Table 1 is for the 64% isomer. Re(1) and Ru(1) are indistinguishable as are Re(2) and Ru(2). In both isomers, the four metal atoms form a butterfly skeleton and a 2-mercaptobenzothiolato ligand is facially located on the convex side of the cluster, bridging the hinge metal atoms through the exocyclic sulfur atom while coordinating to the wingtip rhenium through the nitrogen atom. Both isomers contain a non-crystallographic mirror plane of symmetry passing through the plane of the heterocyclic ring and also containing the wingtip metals of the butterfly. The metal–metal distances are within the expected range in both isomers [16]. We believe that the two isomers are present in solution since the ^{1}H NMR spectrum shows a series of multiplets in the aromatic region, the pattern being too complex for a single species. We have not, however, been able to assign individual resonances and hence the relative amounts of each isomer remain unknown.

Seeking to prepare **4** in higher yields we also carried out the thermolysis of **1** and $Ru_3(CO)_{12}$ in refluxing toluene. Now, however, neither **3** or **4** were generated, rather the major product was a tetranuclear cluster, tentatively characterized as $[Re_2Ru_2(CO)_{12}(\mu_4\text{-}S)(\mu\text{-}C_7H_4NS)(\mu\text{-}C_7H_4NS_2)]$ (**5**) being isolated in 38% yield. We have been unable to grow crystals of **5** suitable for X-ray diffraction analysis and thus this assignment is based solely on spectroscopic and analytical data. Most informatively, the +ve ion FAB mass spectrum shows a peak at m/z 1244 consistent with the formula proposed, together with further ions due to successive loss of twelve

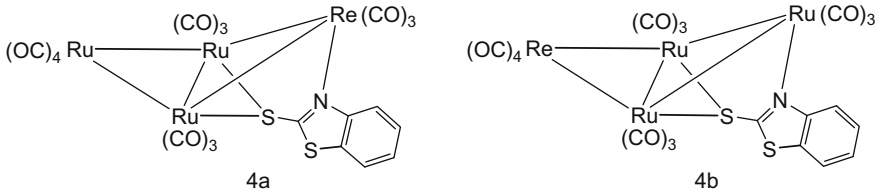

Chart 2.

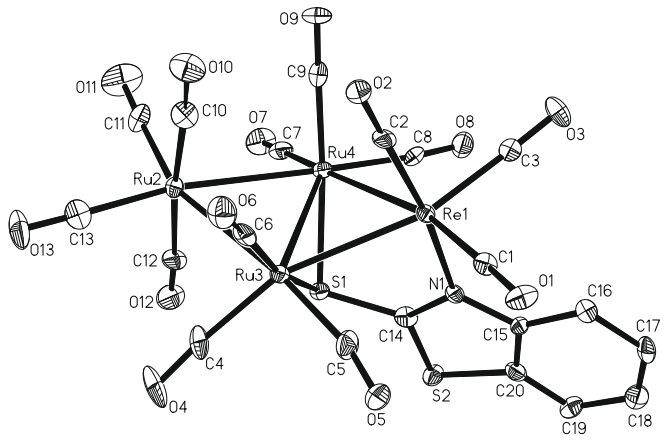

Fig. 3. ORTEP diagram of the molecular structure of $[Ru_3Re(CO)_{13}(\mu_3\text{-}C_7H_4NS_2)]$ (**4**), showing 50% probability thermal ellipsoids. Selected interatomic distances (Å) and angles (°): Ru(3)–Ru(4) 2.7841(11), Re(1)–Ru(3) 2.8610(9), Re(1)–Ru(4) 2.8978(9), Ru(3)–S(1) 2.383(3), Ru(4)–S(1) 2.381(2), Re(1)–N(1) 2.201(8), C(14)–S(1) 1.752(10), Ru(3)–Re(1)–Ru(4) 57.82(2), Ru(4)–Ru(3)–Re(1) 61.75(2), Ru(3)–Ru(4)–Re(1) 60.43(2), S(1)–Ru(4)–Ru(3) 54.28(7), S(1)–Ru(3)–Ru(4) 54.21(6), Ru(4)–S(1)–Ru(3) 71.51(7), N(1)–Re(1)–Ru(3) 87.2(2).

carbonyls. In the IR spectrum only terminal carbonyls are seen and the pattern of which is quite different from those of the tetranuclear mixed rhenium–ruthenium clusters previously reported by Deeming et al. [12] In the ^{1}H NMR spectrum, the observation of four doublets and an equal number of triplets shows the presence of two non-equivalent benzoheterocyclic ligands. We could not, however, differentiate unequivocally between μ-C_7H_4NS and μ-$C_7H_4NS_2$ ligands from the spectrum. A similar situation is seen for the closely related complexes, $[Re_2Ru_2(CO)_{13}(\mu_4\text{-}S)(\mu\text{-}C_5H_4N)(\mu\text{-}C_5H_4NS)]$ [12b] and $[Re_2Fe_2(CO)_{13}(\mu_4\text{-}S)(\mu\text{-}C_5H_4N)(\mu\text{-}C_5H_4NS)]$ [13b], which differ from **5** by the absence of rhenium–rhenium bond and presence of an additional carbonyl ligand.

Treatment of **1** with two equivalents of $Fe_3(CO)_{12}$ in refluxing benzene led to the isolation of triangular mixed-metal complex $[Fe_2Re(CO)_7(\mu\text{-}CO)_3(\mu_3\text{-}C_7H_4NS_2)]$ (**6**) in 23% yield. The IR spectrum shows five terminal carbonyl bands together with an absorption at 1824 cm^{-1} indicating the presence of one or more bridging carbonyls. In order to fully elucidate the structure a single crystal X-ray diffraction study was carried out. An ORTEP diagram of the molecular structure of **6** is depicted in Fig. 4 and selected bond distances and angles are listed in the caption. The molecule comprises a triangular array of one rhenium and two iron atoms with eight terminal carbonyls and two bridging carbonyls and is capped by a triply bridging 2-mercaptobenzothiazolato ligand. One of the bridging carbonyls span the iron–iron vector, while the second bridges an iron–rhenium bond, the M–C distances and M–C–O angles revealing the asymmetric nature of the latter. The 2-mercaptobenzothiazolato ligand bridges the iron–iron edge approximately symmetrically [Fe(1)–S(2) 2.284(2) Å and Fe(2)–S(2) 2.272(2) Å], and also coordinates to rhenium through the nitrogen atom. The rhenium–iron bond lengths [Re(1)–Fe(1) 2.8127(10) Å and Re(1)–Fe(2) 2.8317(11) Å] are in between the metal–metal bond distances found in $Fe_3(CO)_{12}$ (2.660 and 2.558(1) Å) [20] and $Re_2(CO)_{10}$ (3.042(1) Å) [21], but the iron–iron bond length (2.5257(15) Å) is even shorter than the doubly CO-bridged iron–iron edge in $Fe_3(CO)_{12}$. Formation of **6** results from the loss of an iron atom and such behavior is not unexpected.

2.3. Reactivity of $[Os_3Re(CO)_{13}(\mu_3\text{-}C_7H_4NS_2)]$ (**2**) towards PPh_3

Since tetranuclear **2**, the target product of the reaction of **1** with $M_3(CO)_{12}$, was formed in good yields we decided to carry out a preliminary reactivity study in order to ascertain whether simple carbonyl substitution would be selectively directed to a single coordination site at a single metal centre. In this respect it is worth pointing out that the thirteen carbonyls occupy nine different sites and thus in theory simple substitution of a single carbonyl could give rise to eight isomers. Cluster **2** reacts with PPh_3 at room temperature in the presence of Me_3NO to give a mixture of mono- and di-substituted products $[Os_3Re(CO)_{12}(PPh_3)(\mu_3\text{-}C_7H_4NS_2)]$ (**7**) and $[Os_3Re(CO)_{11}(PPh_3)_2(\mu_3\text{-}C_7H_4NS_2)]$ (**8**) respectively formed in 11 and 42% yields. In a separate experiment we showed that **7** converted into **8** when treated with PPh_3 in presence of Me_3NO under similar conditions (Scheme 2).

It was clear from spectroscopic data that both existed as a single isomer. For example, the $^{31}P\{^1H\}$ NMR spectrum of **7** displays only one singlet, while that of **8** shows two singlets, this latter data suggesting that a single metal center was not doubly substituted. On the basis of spectroscopic data however it was not possible to know the exact disposition of the phosphine ligands and hence single crystal X-ray diffraction analyses were carried out for both the compounds. ORTEP diagrams of the molecular structures of **7** and **8** are shown in Figs. 5 and 6, respectively and selected bond angles and distances are listed in the captions. In both the core of the molecule remains essentially unchanged from that in **2**. The single PPh_3 ligand in **7** is bound to the wingtip osmium and occupies an axial coordination site. This is quite surprising since the bulky tertiary phosphines normally occupy equatorial coordination sites of metals, which places them trans to the metal–metal bond. It is also noteworthy that it is bound on the same side of the cluster core as the 2-mercaptobenzothiazolato ligand. We assume that this is a steric preference. In di-substituted **8** the two phosphine ligands are bound to a hinge and wingtip osmium atoms, respectively. Here, however, the phosphine bound to the wingtip osmium occupies an equatorial site lying trans to the Os(1)–Os(2) vector, while that coordinated to a hinge osmium atom also adopts an equatorial position lying trans to the Os(2)–Os(3) vector. Such an arrangement of two phosphine ligands about a triosmium centeris quite common and satisfies the preference to be trans to a metal–metal bond while minimizing steric repulsion between them. The osmium–phosphorus distance of 2.496(2) Å in **7** is considerably longer than those observed in **8** [2.357(1)and2.398(1)Å]. The relative elongation of the former may be a consequence of the need to minimize non-bonded interactions between the benzoheterocycle and phosphine and in accord with this we note that the P(1)Os(1)C(2) axis is tilted away from the benzoheterocyclic ligand.

Table 1
Crystallographic data and structure refinement for **1**, **2**, **4**, **6**, **7** and **8.**

Compound	**1**	**2**	**4**	**6**	**7** · $0.71CH_2Cl_2$	**8**
Empirical formula	$C_{20}H_8N_2O_6Re_2S_4$	$C_{20}H_4NO_{13}Os_3ReS_2$	$C_{20}H_4NO_{13}ReRu_3S_2$	$C_{17}H_4Fe_2NO_{10}ReS_2$	$C_{37}H_{19}NO_{12}Os_3PReS_20.71CH_2Cl_2$	$C_{54}H_{34}NO_{11}Os_3P_2ReS_2$
Formula weight	872.92	1287.2	1019.8	744.23	1581.7	1755.7
Temp (K)	150(2)	150(2)	100(2)	293(2)	100(2)	100(2)
Wavelength (Å)	0.7107	0.7107	1.5418	0.7107	0.7107	0.7107
Crystal system	Monoclinic	Triclinic	Monoclinic	Orthorhombic	Monoclinic	Triclinic
Space group	$C2/c$	$P\bar{1}$	$P2_1/c$	$P2_12_12_1$	$P2_1/c$	$P\bar{1}$
a (Å)	14.343(1)	8.580(1)	9.1775(2)	8.6114(5)	9.186(5)	8.988(3)
b (Å)	11.9707(8)	9.059(2)	8.5897(2)	9.286(1)	24.18(1)	14.802(4)
c (Å)	13.693(1)	17.706(3)	32.7982(6)	26.595(2)	18.90(1)	19.424(5)
α (°)	90	76.174(2)	90	90	90	86.221(4)
β (°)	93.601(3)	81.430(3)	90.984(1)	90	98.011(8)	86.695(4)
γ (°)	90	84.969(3)	90	90	90	76.794(4)
V (Å^3)	2346.3 (3)	1319.5(4)	2585.2(1)	2126.6(3)	4158(4)	2508(1)
Z	4	2	4	4	4	2
D_{calc} (Mg m^{-3})	2.471	3.24	2.62	2.325	2.527	2.325
μ (Mo Kα) (mm^{-1})	10.706	19.194	24.999	7.277	12.332	10.192
F(0 0 0)	1616	1140	1896	1408	2895	1636
Crystal size (mm)	0.25 × 0.08 × 0.08	0.16 × 0.16 × 0.14	0.25 × 0.13 × 0.06	0.40 × 0.12 × 0.12	0.30 × 0.14 × 0.02	0.35 × 0.12 × 0.04
θ range (°)	2.98–30.46	2.35–28.26	2.69–68.06	2.32–25.26	1.38–31.85	1.42–31.97
Index ranges	$15 \leqslant h \geqslant 20$, $-14 \leqslant k \geqslant 16$, $-15 \leqslant l \geqslant 17$	$-11 \leqslant h \geqslant 11$, $-12 \leqslant k \geqslant 11$, $-23 \leqslant l \geqslant 22$	$-10 \leqslant h \geqslant 10$, $0 \leqslant k \geqslant 10$, $0 \leqslant l \geqslant 39$	$0 \leqslant h \geqslant 10$, $-11 \leqslant k \geqslant 3$, $-31 \leqslant l \geqslant 31$	$-13 \leqslant h \geqslant 13$, $0 \leqslant k \geqslant 35$, $0 \leqslant l \geqslant 27$	$-13 \leqslant h \geqslant 13$, $-21 \leqslant k \geqslant 21$, $0 \leqslant l \geqslant 28$
Reflections collected	7188	11 141	21 657	4356	65 510	41 390
Independent reflections (R_{int})	2883 (0.0903)	5922 (0.0336)	4613 (0.0237)	3801 (0.0190)	13 379 (0.0580)	16 069 (0.0321)
Max. and min. transmission	0.481 and 0.294	0.1741 and 0.1492	0.3154 and 0.0622	0.4755 and 0.1589	0.7905 and 0.1193	0.6860 and 0.1247
Data/restraints/parameters	2883/0/155	5922/0/356	4613/0/363	3801/0/298	13 379/0/542	16 069/0/667
Goodness-of-fit (GOF) on F^2	1.019	1.051	1.051	1.02	1.056	1.029
Final R indices [$I > 2\sigma(I)$]	$R_1 = 0.0438$, $wR_2 = 0.1087$	$R_1 = 0.0432$, $wR_2 = 0.1212$	$R_1 = 0.0439$, $wR_2 = 0.1178$	$R_1 = 0.0308$, $wR_2 = 0.0727$	$R_1 = 0.0397$, $wR_2 = 0.0858$	$R_1 = 0.0260$, $wR_2 = 0.0568$
R indices (all data)	$R_1 = 0.0539$, $wR_2 = 0.1154$	$R_1 = 0.0489$, $wR_2 = 0.1274$	$R_1 = 0.0440$, $wR_2 = 0.1179$	$R_1 = 0.0406$, $wR_2 = 0.0754$	$R_1 = 0.0560$, $wR_2 = 0.0904$	$R_1 = 0.0335$, $wR_2 = 0.0591$
Largest difference in peak and hole (e Å^{-3})	3.679 and −3.386	2.136 and −4.414	1.541 and −1.427	0.747 and −1.835	2.254 and −2.812	1.869 and −1.215

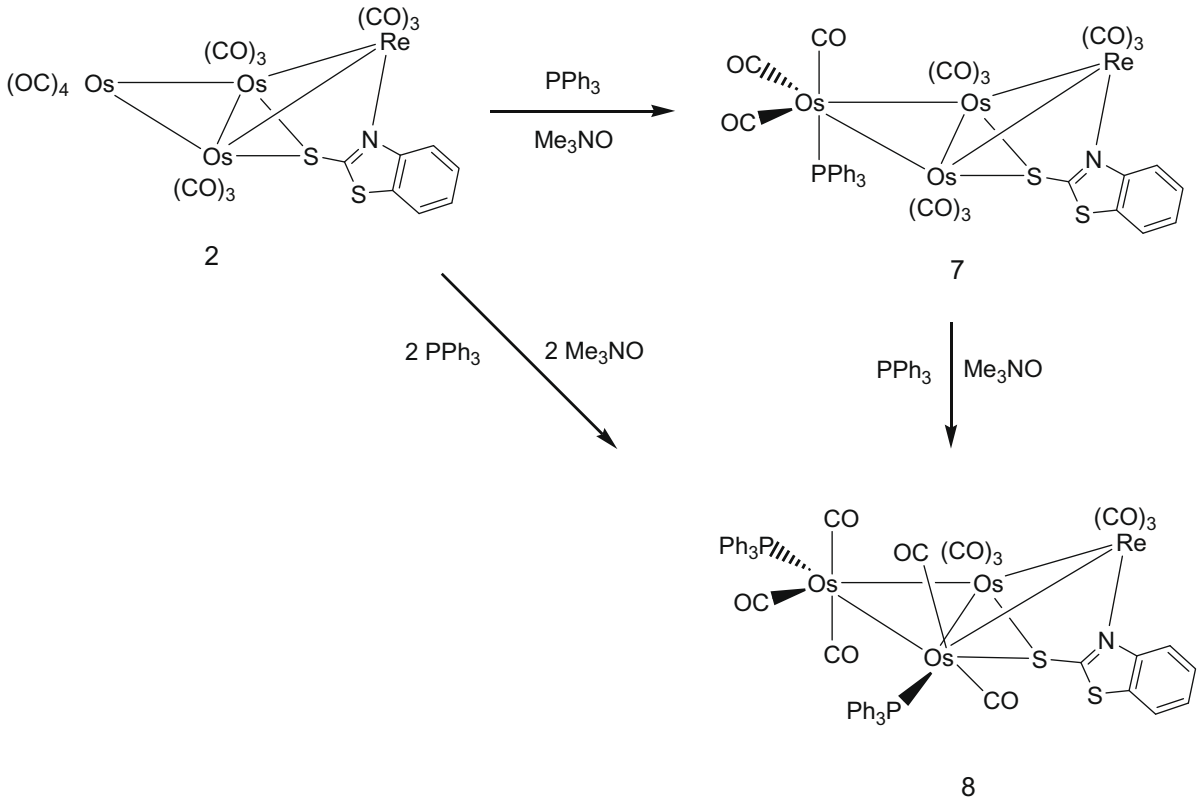

Scheme 2.

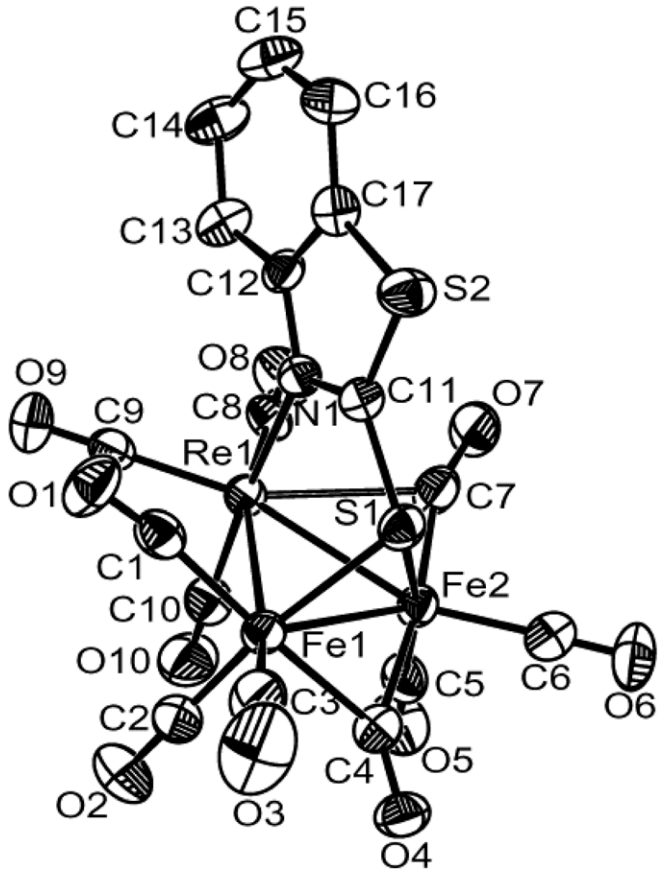

Fig. 4. ORTEP diagram of the molecular structure of $[Fe_2Re(CO)_8(\mu\text{-}CO)_2(\mu_3\text{-}C_7H_4NS_2)]$ (**6**), showing 35% probability thermal ellipsoids. Selected interatomic distances (Å) and angles (°): Re(1)–N(1) 2.209(6), Re(1)–Fe(1) 2.8127(10), Re(1)–Fe(2) 2.8317(11), Fe(1)–Fe(2) 2.5257(15), Fe(1)–S(2) 2.284(2), Fe(2)–S(2) 2.272(2), Re(1)–C(4) 2.595(8), Re(1)–C(10) 2.723(9), Fe(1)–C(4) 1.855(9), Fe(1)–C(7) 1.953(8), Fe(2)–C(10) 1.841(9), Fe(2)–C(7) 1.986(7), C(2)–Re(1)–N(1) 175.4(3), N(1)–Re(1)–Fe(1) 86.52(14), Fe(1)–Re(1)–Fe(2) 53.16(3), S(2)–Fe(1)–Fe(2) 56.11(6), Fe(2)–Fe(1)–Re(1) 63.81(3), S(2)–Fe(2)–Fe(1) 56.57(6), Fe(1)–Fe(2)–Re(1) 63.03(3), Fe(2)–S(2)–Fe(1) 67.32(7), Fe(1)–C(4)–Re(1) 76.4(3), Fe(1)–C(7)–Fe(2) 79.8(3), Fe(2)–C(10)–Re(1) 73.9(9).

3. Conclusions

In summary, we present here a synthetic approach towards bimetallic clusters taking advantage of the relatively weak rhenium–sulfur bond in **1**. We believe that this generates transient $[Re(CO)_3(S_2NC_7H_4)]$ fragments which in turn then react with Group 8 trimetallic carbonyls. In the case of the lightly-stabilized $[Os_3(CO)_{10}(MeCN)_2]$ this resulted in the relatively clean formation of tetranuclear $[Os_3Re(CO)_{13}(\mu_3\text{-}C_7H_4NS_2)]$ (**2**) with the anticipated butterfly arrangement of metal atoms. More forcing conditions were required for the reaction with $Ru_3(CO)_{12}$ and while this lead to the generation of some of the desired tetranuclear product, other species resulting from transfer of the 2-mercaptobenzothiazolato ligand from rhenium to ruthenium and carbon–sulfur bond cleavage meant that this route was not perused further. With $Fe_3(CO)_{12}$ the relatively weak nature of the iron–iron bonds became a factor and no tetranuclear species could be isolated. Rather, trinuclear $[Fe_2Re(CO)_8(\mu\text{-}CO)_2(\mu_3\text{-}C_7H_4NS_2)]$ (**6**) was isolated. Its mode of formation remains unclear but it is tempting to suggest that the desired tetranuclear cluster was initially formed but later scission of an $Fe(CO)_4$ fragment proved facile. Our preliminary reactivity study of **2** towards PPh_3 shows that while there is a high degree of selectivity in carbonyl substitution of heterometallic clusters, the precise product(s) generated can be difficult to predict. Thus we see that in the two products isolated here, the phosphine in each case occupies a unique coordination site the reasons for which are not always easy to determine. Further studies designed to probe the scope and broader applications of this approach towards mixed-metal clusters and their selective reactivity patterns are in currently in progress in our laboratories.

4. Experimental

All reactions were performed under a dry oxygen-free nitrogen atmosphere using standard Schlenk techniques. Reagent grade solvents were freshly distilled from appropriate drying agents prior to use. Infrared spectra were recorded on a Shimadzu FTIR spectrophotometer. NMR spectra were recorded on a Bruker DPX 400 instrument. Elemental analyses were performed by Microanalytical Laboratories, University College London. Fast atom bombardment mass spectra were obtained on a JEOL SX-102 spectrometer using 3-nitrobenzyl alcohol as matrix and CsI as calibrant. The parent carbonyls ($Re_2(CO)_{10}$, $Fe_3(CO)_{12}$, $Ru_3(CO)_{12}$, $Os_3(CO)_{12}$) were purchased from Strem Chemicals Inc. and used without further purification. $Me_3NO{\cdot}2H_2O$ was purchased from Lancaster and water was removed using a Dean-Stark apparatus by azeotropic distillation from benzene and the anhydrous Me_3NO was stored under nitrogen. 2-Mercaptobenzothiazole and triphenylphosphine were purchased from Sigma-Aldrich Chemical Company and used as received. $[Os_3(CO)_{10}(NCMe)_2]$ was prepared according to literature procedure [22].

4.1. Preparation of $[Re_2(CO)_6(\mu\text{-}S_2NC_7H_4)_2]$ (1)

A CH_2Cl_2 solution (20 mL) of $Re_2(CO)_{10}$ (200 mg, 0.306 mmol), 2-mercaptobenzothiazole (103 mg, 0.616 mmol) and Me_3NO (47 mg, 0.625 mmol) was stirred at 25 °C for 72 h. The solution was filtered through a short column (2 cm) of silica gel to remove excess Me_3NO. The solvent was removed under reduced pressure and the residue chromatographed by TLC on silica gel. Elution with hexane/CH_2Cl_2 (4:1, v/v) gave $[Re_2(CO)_6(\mu\text{-}S_2NC_7H_4)_2]$ (**1**) (176 mg, 66%) as yellow crystals after recrystallization from hexane/CH_2Cl_2 at 25 °C. Spectral data for **1**: Anal. Calc for $C_{20}H_8N_2O_6Re_2S_4$: C, 27.52; H, 0.93; N, 3.21. Found: C, 27.79; H, 1.07; N, 3.31%. IR (ν_{CO}, CH_2Cl_2): 2042 (s), 2027 (vs), 1925 (s,br) cm^{-1}. ^1H NMR ($CDCl_3$, 25 °C): δ 7.68 (d, J = 8.4 Hz, 1H), 7.55 (m, 2H), 7.30 (d, J = 8.4 Hz, 1H). FAB-MS: m/z 872 [M^+].

4.2. Reaction of **1** with $[Os_3(CO)_{10}(NCMe)_2]$

A benzene solution (50 mL) of $[Os_3(CO)_{10}(NCMe)_2]$ (ca. 220 mg, 0.236 mmol) and **1** (100 mg, 0.114 mmol) was heated to reflux for 2 h. Work-up and chromatographic separation as above afforded $[Os_3Re(CO)_{13}(\mu_3\text{-}C_7H_4NS_2)]$ (**2**) (179 mg, 61%) as red crystals after recrystallization from hexane/CH_2Cl_2 at 25 °C. Spectral data for **2**: Anal. Calc. for $C_{20}H_4NO_{13}Os_3ReS_2$: C, 18.66; H, 0.31; N, 1.09. Found: C, 18.98; H, 0.37; N, 1.17%. IR (ν_{CO}, CH_2Cl_2): 2110 (m), 2045 (vs), 2027 (m), 2014 (m), 1968 (w) cm^{-1}. ^1H NMR ($CDCl_3$, 25 °C): δ 8.39 (d, J = 8.4 Hz, 1H), 8.30 (d, J = 8.4 Hz, 1H), 7.99 (t, J = 8.4 Hz, 1H), 7.77 (t, J = 8.4 Hz, 1H). FAB-MS: m/z 1288 [M^+].

4.3. Reaction of **1** with $Ru_3(CO)_{12}$ at 80 °C

A benzene solution (20 mL) of $Ru_3(CO)_{12}$ (100 mg, 0.156 mmol) and **1** (70 mg, 0.080 mmol) was heated to reflux for 3 h. A similar workup described as above developed four bands on TLC plates. The first band was unreacted $Ru_3(CO)_{12}$. The second and third bands gave $[Ru_3(CO)_9(\mu\text{-}H)(\mu_3\text{-}C_7H_4NS_2)]$ (**3**) (16 mg, 14%) as red

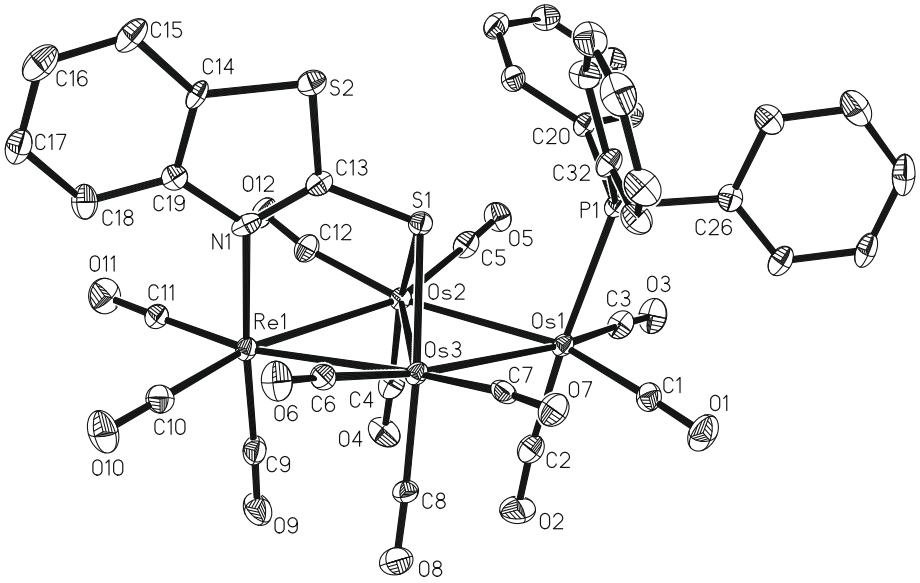

Fig. 5. ORTEP diagram of the molecular structure of $[Os_3Re(CO)_{12}(PPh_3)(\mu_3\text{-}C_7H_4NS_2)]$ (**7**), showing 50% probability thermal ellipsoids. Selected interatomic distances (Å) and angles (°): Os(1)–Os(2) 2.8884(12), Os(1)–Os(3) 2.9214(12), Os(2)–Os(3) 2.7558(12), Os(2)–Re(1) 2.9338(12), Os(3)–Re(1) 2.9694(12), Os(2)–S(1) 2.4031(18), Os(3)–S(1) 2.3904(18), Re(1)–N(1) 2.215(5), Os(1)–P(1) 2.496(2), Os(2)–Os(1)–Os(3) 56.629(15), Os(3)–Os(2)–Os(1) 62.29(3), Os(3)–Os(2)–Re(1) 62.83(3), Os(2)–Os(3)–Os(1) 61.08(3), Os(1)–Os(2)–Re(1) 124.186(18), Os(2)–Os(3)–Re(1) 61.52(2), Os(1)–Os(3)–Re(1) 121.71(2), Os(2)–Re(1)–Os(3) 55.65(2), Os(3)–S(1)–Os(2) 70.19(5), S(1)–Os(2)–Os(3) 54.69(4), S(1)–Os(2)–Os(1) 75.71(4), S(1)–Os(3)–Os(2) 55.12(4), S(1)–Os(3)–Os(1) 75.24(4), C(9)–Re(1)–N(1) 175.8(2), C(2)–Os(1)–P(1) 175.3(2), P(1)–Os(1)–Os(3) 103.15(4).

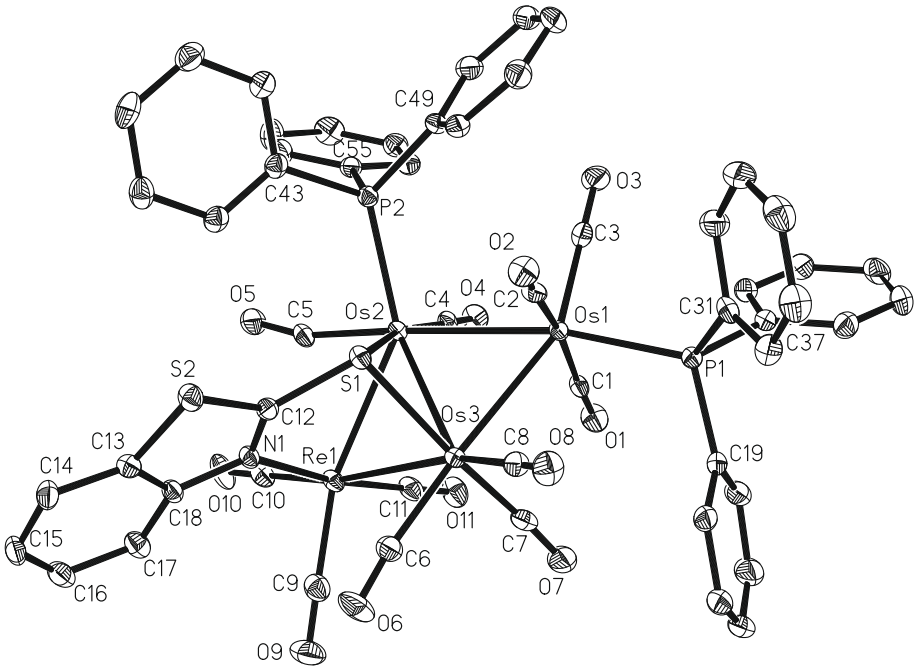

Fig. 6. ORTEP diagram of the molecular structure of $[Os_3Re(CO)_{11}(PPh_3)_2(\mu_3\text{-}C_7H_4NS_2)]$ (**8**), showing 50% probability thermal ellipsoids. Selected interatomic distances (Å) and angles (°): Os(1)–Os(2) 2.9028(8), Os(1)–Os(3) 2.8542(6), Os(2)–Os(3) 2.8117(7), Os(2)–Re(1) 2.9058(5), Os(3)–Re(1) 2.9149(7), Os(2)–S(1) 2.4140(9), Os(3)–S(1) 2.4275(10), Re(1)–N(1) 2.214(3), Os(1)–P(1) 2.3570(11), Os(2)–P(2) 2.3982(10), Os(3)–Os(1)–Os(2) 58.462(15), Os(3)–Os(2)–Os(1) 59.904(7), Os(3)–Os(2)–Re(1) 61.277(16), Os(2)–Os(3)–Os(1) 61.634(19), Os(1)–Os(2)–Re(1) 114.465(13), Os(2)–Os(3)–Re(1) 60.953(8), Os(1)–Os(3)–Re(1) 115.692(16), Os(2)–S(1)–Os(3) 71.01(3), C(11)–Re(1)–N(1) 171.03(13), S(1)–Os(2)–Os(3) 54.72(2), S(1)–Os(2)–Os(1) 86.40(2), S(1)–Os(3)–Os(2) 54.27(2), P(1)–Os(1)–Os(2) 168.80(2), P(1)–Os(1)–Os(3) 111.50(3), P(2)–Os(2)–S(1) 96.01(4), P(2)–Os(2)–Os(3) 143.51(2), P(2)–Os(2)–Os(1) 101.43(2).

crystals and $[Ru_3Re(CO)_{13}(\mu_3\text{-}C_7H_4NS_2)]$ (**4**) (37 mg, 23%) as pink crystals after recrystallization from hexane/CH_2Cl_2 at 4 °C. Spectral data for **3**: Anal. Calc. for $C_{16}H_5NO_9Ru_3S_2$: C, 26.60; H, 0.69; N, 1.94. Found: C, 26.98; H, 0.81; N, 2.05%. ^{1}H NMR ($CDCl_3$, 25 °C): δ 7.81 (d, J = 8.0 Hz, 1H), 7.73 (d, J = 8.0 Hz, 1H), 7.66 (d, J = 8.0 Hz, 1H), 7.45 (d, J = 8.0 Hz, 1H), −12.88 (br,s, J = 8.4 Hz, 1H). FAB-MS: m/z 722 [M^+]. Spectral data for **4**: Anal. Calc. for $C_{20}H_4NO_{13}Ru_3ReS_2$: C, 23.55; H, 0.39; N, 1.37. Found: C, 23.91; H, 0.44; N, 1.43%. IR (ν_{CO}, CH_2Cl_2): 2103 (m), 2094 (w), 2061 (m), 2044 (vs), 2033 (s), 2012 (m), 1977 (m,br), 1921 (w) cm^{-1}. ^{1}H NMR ($CDCl_3$, 25 °C): δ 8.24 (d, J = 8.4 Hz, 2H), 7.87 (m, 3H), 7.73 (m, 4H), 7.60 (m, 2H), 7.54 (m, 1H).

4.4. Reaction of **1** with $Ru_3(CO)_{12}$ at 110 °C

To a toluene solution (20 mL) of $Ru_3(CO)_{12}$ (73 mg, 0.114 mmol) was added **1** (100 mg, 0.114 mmol) and the mixture was heated to reflux for 30 min. The solvent was removed under vacuum and the residue separated by TLC on silica gel. Elution with hexane/acetone (9:1, v/v) afforded $[Re_2Ru_2(CO)_{12}(\mu_4\text{-}S)(\mu\text{-}C_7H_4NS)(\mu\text{-}C_7H_4NS_2)]$ (**5**) (54 mg, 38%) as orange crystals after recrystallization from hexane/CH_2Cl_2 at 4 °C. Spectral data for **5**: Anal. Calc. for $C_{26}H_8N_2O_{12}Re_2Ru_2S_4$: C, 25.12; H, 0.65; N, 2.25. Found: C, 25.46; H, 0.72; N, 2.31%. IR (ν_{CO}, CH_2Cl_2): 2051 (vs), 2033 (m), 2006 (s), 1977 (s,br), 1923 (m,br), 1889 (m,br) cm^{-1}. ^1H NMR ($CDCl_3$, 25 °C): δ 8.55 (d, J = 8.4 Hz, 1H), 8.02 (d, J = 8.4 Hz, 1H), 7.89 (d, J = 8.4 Hz, 1H), 7.86 (d, J = 8.4 Hz, 1H), 7.62 (t, J = 8.4 Hz, 1H), 7.53 (t, J = 8.4 Hz, 1H), 7.43 (t, J = 8.4 Hz, 1H), 7.38 (t, J = 8.4 Hz, 1H). FAB-MS: m/z 1244 [M^+].

4.5. Reaction of **1** with $Fe_3(CO)_{12}$

1 (100 mg, 0.114 mmol) was added to a benzene solution (20 mL) of $Fe_3(CO)_{12}$ (116 mg, 0.230 mmol) and the mixture was heated to reflux for 1 h. The solvent was removed by rotary evaporation and the residue chromatographed by TLC on silica gel. Elution with hexane/acetone (4:1, v/v) developed one major and several minor bands. The major band afforded $[Fe_2Re(CO)_8(\mu\text{-}CO)_2(\mu_3\text{-}C_7H_4NS_2)]$ (**6**) (39 mg, 23%) as red crystals after recrystallization from hexane/CH_2Cl_2 at 4 °C while the minor bands were too small for characterization. Spectral data for **6**: Anal. Calc. for $C_{17}H_4Fe_2NO_{10}ReS_2$: C, 27.43; H, 0.54; N, 1.88. Found: C, 27.72; H, 0.58; N, 1.92%. IR (ν_{CO}, CH_2Cl_2): 2078 (m), 2043 (s), 2026 (vs), 2010 (m), 1950 (m, br), 1812 (m, br) cm^{-1}. ^1H NMR ($CDCl_3$, 25 °C): δ 8.26 (d, J = 8.0 Hz, 1H), 7.87 (d, J = 8.0 Hz, 1H), 7.83 (t, J = 8.0 Hz, 1H), 7.63 (t, J = 8.0 Hz, 1H).

4.6. Reaction of **2** with PPh_3

To a CH_2Cl_2 solution (20 mL) of **2** (100 mg, 0.078 mmol) and PPh_3 (41 mg, 0.156 mmol) was added dropwise a CH_2Cl_2 solution (10 mL) of Me_3NO (12 mg, 0.159 mmol) and the mixture was stirred at 25 °C for 1 h. The solvent was removed in vacuo and the residue separated by TLC on silica gel. Elution with hexane/acetone (4:1, v/v) developed two red bands. The minor band afforded $[Os_3Re(CO)_{12}(PPh_3)(\mu_3\text{-}C_7H_4NS_2)]$ (**7**) (13 mg, 11%) while the major band gave $[Os_3Re(CO)_{11}(PPh_3)_2(\mu_3\text{-}C_7H_4NS_2)]$ (**8**) (57 mg, 42%) as red crystals after recrystallization from hexane/CH_2Cl_2 at 4 °C. Spectral data for **7**: Anal. Calc. for $C_{37}H_{19}NO_{12}Os_3PReS_2$: C, 29.21; H, 1.26; N, 0.92. Found: C, 29.49; H, 1.34; N, 0.99%. IR (ν_{CO}, CH_2Cl_2): 2076 (m), 2027 (vs), 2004 (m), 1945 (m,br) cm^{-1}. ^1H NMR ($CDCl_3$, 25 °C): δ 8.41 (d, J = 10.8 Hz, 1H), 7.86 (d, J = 10.8 Hz, 1H), 7.78 (t, J = 10.8 Hz, 1H), 7.62 (t, J = 10.8 Hz, 1H), 7.52–7.33 (m, 30H). $^{31}P\{^1H\}$ NMR ($CDCl_3$, 25 °C): δ = 7.72 (s). Spectral data for **8**: Anal. Calcd for $C_{54}H_{34}NO_{11}Os_3P_2ReS_2$: C, 36.94; H, 1.95; N, 0.78. Found: C, 37.25; H, 2.10; N, 0.84%. IR (ν_{CO}, CH_2Cl_2): 2056 (m), 2016 (vs), 1997 (sh), 1979 (s), 1960 (m), 1939 (m,br), 1923 (m,br) cm^{-1}. ^1H NMR ($CDCl_3$, 25 = °C): δ 8.33 (d, J = 10.8 Hz, 1H), 7.81 (d, J = 10.8 Hz, 1H), 7.73 (t, J = 10.8 Hz, 1H), 7.53 (t, J = 10.8 Hz, 1H), 7.46–7.29 (m, 30H). $^{31}P\{^1H\}$ NMR ($CDCl_3$, 25 °C): δ = 6.06 (s, 1P), −7.31 (s, 1P). FAB-MS: m/z 1756 [M^+].

4.7. Conversion of 7 to 8

Me_3NO (1 mg, 0.013 mmol) was added dropwise to a CH_2Cl_2 solution (15 mL) of **7** (20 mg, 0.013 mmol) and PPh_3 (4 mg, 0.015 mmol) and the mixture was stirred at 25 °C for 45 min. A similar chromatographic separation and work up described as above gave **8** (18 mg, 81%).

5. X-ray crystallography

Single crystals were mounted on fibers and diffraction data collected at low temperature (see Table 1) on Nonius Kappa CCD (1), Bruker APEX2 CCD (2), Bruker APEX2 CCD (4, 7, 8), Enraf Nonius TurboCAD4 (6) diffractometers using Mo Kα radiation (λ = 0.71073 Å). Data collection, indexing and initial cell refinements were all done using SMART [23] software. Data reduction was accomplished with SAINT [24] software and the DIFABS [25] and SADABS [26] programs were used to apply empirical absorption corrections. The structures were solved by direct methods [27] and refined by full matrix least-squares [28]. Except in **2**, all non-hydrogen atoms were refined anisotropically and hydrogen atoms were included using a riding model. Scattering factors were taken from International Tables for X-ray crystallography [29]. Additional details of data collection and structure refinement are given in Table 1.

6. Supplementary material

CCDC 711555, 711556, 711557, 715807, 295429 and 295428 contain the supplementary crystallographic data for this paper. These data can be obtained free of charge from The Cambridge Crystallographic Data Centervia www.ccdc.cam.ac.uk/data_request/cif.

Acknowledgements

This research has been sponsored by the Ministry of Science and Information & Communication Technology, Government of the People's Republic of Bangladesh.

References

[1] R.D. Adams, in: E.W. Abel, F.G.A. Stone, G. Wilkinson (Eds.), Comprehensive Organometallic Chemistry II, vol. 10, Elsevier, Oxford, 1995, p. 1.
[2] Y. Chi, D.K. Hwang, in: E.W. Abel, F.G.A. Stone, G. Wilkinson (Eds.), Comprehensive Organometallic Chemistry II, vol. 10, Elsevier, Oxford, 1995, p. 85.
[3] P. Braunstein, J. Rosé, in: E.W. Abel, F.G.A. Stone, G. Wilkinson (Eds.), Comprehensive Organometallic Chemistry II, vol. 10, Elsevier, Oxford, 1995, p. 351.
[4] Catalysis by Di- and Polynuclear Metal Cluster Complexes, in: R.D. Adams, F.A. Cotton (Eds.), Wiley, VCH, Chichester, 1998.
[5] (a) R.D. Adams, T.S. Barnard, Organometallics 17 (1998) 2885;
(b) R.D. Adams, T.S. Barnard, Organometallics 17 (1998) 2567;
(c) R.D. Adams, T.S. Barnard, Z. Li, W. Wu, J.H. Yamamoto, J. Am. Chem. Soc. 116 (1994) 9103.
[6] (a) E.L. Muetterties, Science 196 (1977) 839;
(b) B.F.G. Johnson, M. Gallup, Y.V.J. Roberts, Mol. Catal. 86 (1994) 51.
[7] M.E. Broussard, B. Juma, S.G. Train, W.-J. Peng, S.A. Laneman, G.G. Stanley, Science 260 (1993) 1784.
[8] (a) H. Ishii, M. Goyal, M. Ueda, K. Takeuchi, M. Asai, J. Mol. Catal. A 148 (1999) 249;
(b) E. Sappa, A. Tiripicchio, A.J. Carty, G.E. Toogood, Prog. Inorg. Chem. 35 (1987) 437.
[9] (a) A. Fusi, R. Ugo, R. Psaro, P. Braunstein, J. Dehand, J. Mol. Catal. 16 (1982) 217;
(b) V. Ferrand, G. Süss-Fink, A. Neels, H. Stoeckli-Evans, J. Chem. Soc., Dalton Trans. (1998) 3825.
[10] P. Braunstein, J. Rosé, in: P. Braunstein, L.A. Oro, P.R. Raithby (Eds.), Metal Clusters in Catalysis, vol. 2, Wiley-VCH, Weinheim, Germany, 1999, p. 616.
[11] (a) E.K. van den Beuken, B.L. Feringa, Tetrahedron 54 (1998) 12985;
(b) P. Kalck, Polyhedron 7 (1988) 2441–2450.
[12] (a) A.J. Deeming, M. Karim, N.I. Powell, K.I. Hardcastle, Polyhedron 9 (1990) 623;
(b) B. Cockerton, A.J. Deeming, M. Karim, K. Hardcastle, J. Chem. Soc., Dalton Trans. (1991) 431.
[13] (a) A.J. Deeming, M. Karim, P.A. Bates, M.B. Hursthouse, Polyhedron 7 (1988) 1401;
(b) S. Ghosh, K.N. Khanam, G.M.G. Hossain, D.T. Haworth, S.V. Lindeman, G. Hogarth, S.E. Kabir, New J. Chem., accepted for publication.
[14] N. Begum, S.E. Kabir, G.M.G. Hossain, A.F.M.M. Rahman, E. Rosenberg, Organometallics 24 (2005) 266.

[15] S. Ghosh, S.E. Kabir, S. Pervin, G.M.G. Hossain, D.T. Haworth, S.V. Lindeman, T.A. Siddiquee, D.W. Bennett, H.W. Roesky, Z. Anorg. Allg. Chem. 635 (2009) 76.
[16] S.E. Kabir, A.K. Raha, S. Pervin, S. Ghosh, G.M.G. Hossain, D.T. Haworth, S.V. Lindeman, T.A. Siddiquee, D.W. Bennett, L. Salassa, H.W. Roesky, J. Chem. Soc., Dalton Trans. (2009) 3510.
[17] S.E. Kabir, J. Alam, S. Ghosh, K. Kundu, G. Hogarth, D.A. Tocher, G.M.G. Hossain, H.W. Roesky, J. Chem. Soc., Dalton Trans. (2009) 4458.
[18] E.G. Tulsky, J.R. Long, Inorg. Chem. 40 (2001) 6990.
[19] S. Jeannin, Y. Jeannin, G. Lavigne, Inorg. Chem. 17 (1978) 2103.
[20] P.R. Raithby, Transition Metal Clusters, in: B.F.G. Johnson (Ed.), Wiley, VCH, 1980, p. 25 (Chapter 2).
[21] D.W. Prest, M.J. Mays, P.R. Raithby, A.G. Orpen, J. Chem. Soc., Dalton Trans. (1982) 737.
[22] B.F.G. Johnson, J. Lewis, D.A. Pippard, J. Chem. Soc., Dalton Trans. (1981) 407.
[23] SMART Version 5.628, Bruker AXS, Inc., Madison, WI, 2003.
[24] SAINT Version 6.36, Bruker AXS, Inc., Madison, WI, 2002 .
[25] N. Walker, D. Stuart, Acta Crystallogr., Sect. A 39 (1983) 158.
[26] Sheldrick, SADABS Version 2.10, University of Göttingen, 2003.
[27] Program XS from SHELXTL package, V. 6.12, Bruker AXS, Inc., Madison, WI, 2001.
[28] A. Fom, Program XL from SHELXTL package, V. 6.12, Bruker AXS, Inc., Madison. WI, 2001.
[29] A.J.C. Wilson, Ed. International Tables for X-ray Crystallography, Volume C; Kynoch, Academic Publishers, Dordrecht, 1992, Tables 6.1.1.4 (pp. 500–502) and 4.2.6.8 (pp. 219–222).